Controllable Shock and Vibration Dampers Based on Magnetorheological Fluids

ULRICH LANGE*, SVETLA VASSILEVA**, LOTHAR ZIPSER*
*Centre of Applied Research and Technology
at the University of Applied Sciences Dresden
01069 Dresden, Friedrich-List-Platz 1
GERMANY
**Institute of Control and Systems Research
Bulgarian Academy of Sciences
Akad. G. Bontchev str., bl. 2, P.O.Box 79, 1113 Sofia
BULGARIA

Abstract: Innovative magnetorheological dampers (MR dampers) for shock and vibration damping, based on magnetorheological fluids (MRFs), are described. Important fields of their application are loading processes, impact dampers in security systems as well as vibration dampers for machines and cars. Various models for describing the MR dampers are discussed. The characteristic feature of the MR dampers is their electromagnetic controllability in a fast and energy-efficient way. Selected types of controllers for intelligent damping of motions and their behaviour in connection with MR dampers are presented.

Key-Words: magnetorheological fluids, controllable dampers, vibration damping

1 Introduction

Conventional dampers are sufficient for usual applications. For sophisticated ones, e.g. the transportation of dangerous or vibration-sensitive goods, innovative dampers with a controlled behaviour are required. Furthermore, due to their feedback control, disturbances like temperature, friction etc. have no influence on the desired behaviour.

New developments show the smart applicability of magnetorheological fluids for designing efficient controlled dampers. Dampers based on MRFs generate damping forces, which are quickly and continuously modifiable in a wide range by a magnetic field. After a short description of the principles of MRFs, two MR dampers and their controlled behaviour are presented.

2 Magnetorheological Fluids

Magnetorheological fluids are suspensions of soft-magnetic particles about 1 to 5 µm in diameter suspended in special oils [1],[2],[3]. The particles are covered with a thin non-magnetic film which prevents agglomeration. The weight percentage of the particles in the suspension is about 80 % at a total density of about 3 g/cm^3. A raster-electron microscope (REM) view of the particles is shown in Fig. 1. Without a magnetic field the particles are statistically distributed. Under the influence of a magnetic field the particles line up in chains. This behaviour is the "magnetorheological effect". If an external force or pressure are applied, the chains are deformed as shown in Fig. 2 [4]. In the shear mode the chains resist the displacement of the bordering plates. In the flow mode the chains are deformed and resist the applied pressure. In the squeeze mode the chains prevent the draining away of the fluid.

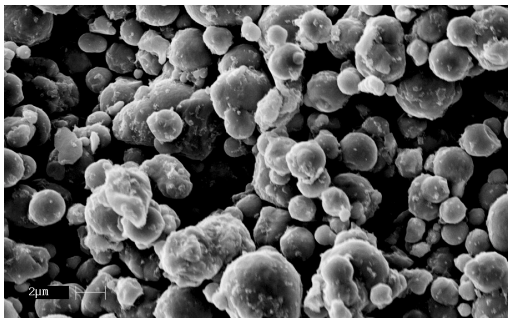

Fig. 1: REM-view of ferromagnetic particles of a typical MRF

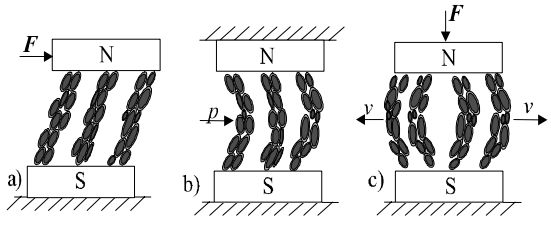

Fig. 2: Stress modes of MRFs
a) shear mode, b) flow mode, c) squeeze mode

Most interesting for dampers is the flow mode. In this case under the influence of a magnetic field the MRF changes its flow behaviour from Newtonian to Bingham characteristics. The Bingham flow is described as [5]

$$\tau(B,\dot{\gamma},\eta) = \tau_f(B) + \eta_B \cdot \dot{\gamma} \qquad (1)$$

with the shear stress τ, the yield point τ_f, the magnetic flux density B, the Bingham viscosity η_B and the rate of shear $\dot{\gamma}$. A graphical presentation of (1) is given in Fig. 3.

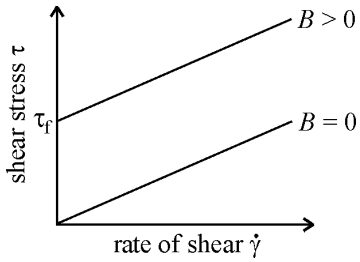

Fig. 3: Graphical presentation of the Bingham eq. (1)

Without a magnetic field at $B = 0$ the MRF is a conventional Newtonian fluid. For $B > 0$ the MRF is a Bingham fluid, with the result that a yield point τ_f emerges. For values $\tau < \tau_f$ the MRF behaves like a solid (area 1 in Fig. 4). Only at higher shear stresses $\tau > \tau_f$ does the MRF behave like a fluid (area 2 in Fig. 4) [6]. The maximal tested yield point τ_f is about 100 kPa at a magnetic flux density $B \approx 1$ T [7].
This interesting viscoelastic behaviour can be used in dampers for the controlled damping of motions.

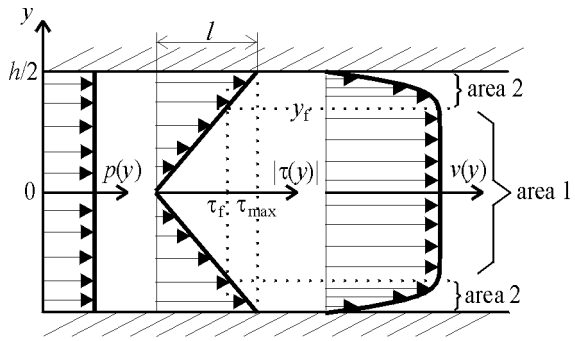

Fig. 4: Distributions of pressure $p(y)$, shear stress $\tau(y)$ and flow velocity $v(y)$ across a tube

3 Shock Damper

For investigating the magnetorheological effect in shock damping a novel MR damper was constructed as a robust pre-production type (Fig. 5). It consists of two interconnected cylinders filled with MRF and uses the flow mode. Due to an external force F_{ext} the pistons are moving with the velocity v (Fig. 6). The displacement s is measured by a noncontact sensor. At the interconnecting channel with a cross section of 4 x 20 mm^2 acts a magnetic flux density B, induced by an electromagnet. Thereby a damping force $F_D(B)$ is generated. In consequence of this the velocity v is controllable between zero and the maximal velocity v_0 at $B = 0$. An electric power of some watts only is required to provide a damping force of about 1 kN.
The transfer function $G(s)$ between the output velocity v and the input current I_{set} is approximately

$$G(s) = -v_0 \frac{k}{1+sT_1} e^{-sT_d} \qquad (2)$$

with time constant of the electromagnet $T_1 = 2.2$ ms and time delay $T_d = 13$ ms. The main part of T_d is due to the inertia force of the moved masses.

Fig. 5: Prototype of an MR shock damper

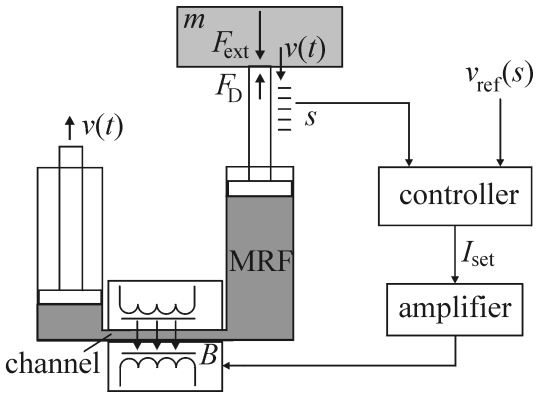

Fig. 6: Scheme of an MR shock damper

In the simplest version a PI-controller influences the current I_{set}. The PI-controller provides a stable closed loop control and a transient time T_t of about 500 ms for the desired output value achievement. In Fig. 8 a

the reference signal v_{ref} is increased from 0 to 20 mm/s at t = 2 s. The transient behaviour is characterised by a large overshot of the velocity v.

For time-critical applications it is necessary to consider the time delay T_d. In this case a predictive controller should improve the behaviour of the system in comparison with a PI-controller. A Smith-Predictor $K(s)$ (Fig. 7) contains a model of the system $G(s)$, separated in a block $\tilde{G}(s)$ without time delay, and a block containing the time delay T_d in the frequency domain - e^{-sT_d}. In the block diagram a feedback for the output signal U of the controller K_{Pr} with evasion of the time delay T_d is shown. Therewith the Smith-Predictor should be faster concerning to changes of the reference signal W.

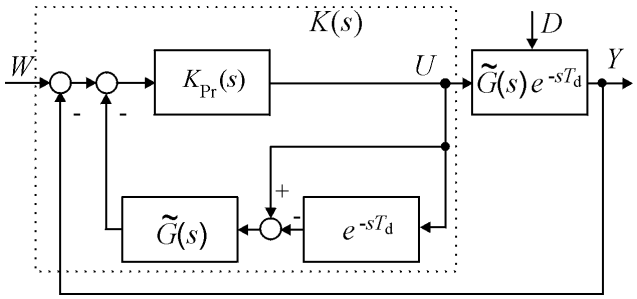

Fig. 7: Block diagram of a Smith-Predictor

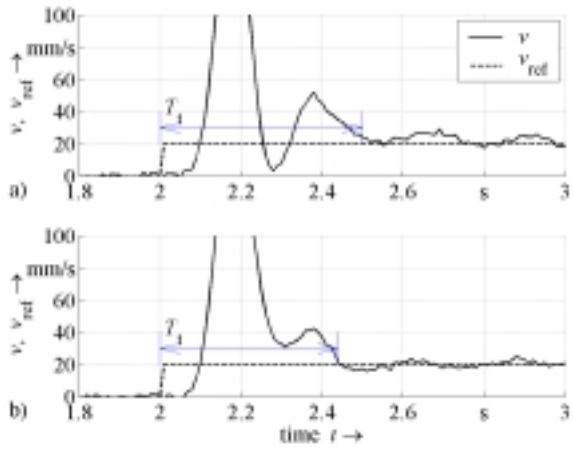

Fig. 8: Step response of the shock damper,
a) PI-controlled, b) controlled with Smith-Predictor

The step response of the velocity v of the shock damper controlled with the Smith-Predictor (Fig. 8 b) follows the reference signal v_{ref} more precisely, with smaller oscillations and somewhat faster ($T_t \approx 440$ ms) than the velocity v of the PI-controlled shock damper (Fig. 8 a).

In order to minimise the uncertainties associated with the real system (Fig. 5) in contrast to (2), expert knowledge and fuzzy design techniques were implemented for two different fuzzy logic controller (FLC) designs: the Mamdani-type and the Takagi-Sugeno-type [8]. In general, FLCs are knowledge-based controllers with rule base, expressed in form of linguistic terms and rules. Fig. 9 shows the basic structure of an FLC with the main stages of an FLC design: fuzzyfication of crisp data into fuzzy sets, inference mechanism, involved in the rule base providing the rules control, defuzzyfication or conversion of the output of fuzzy inference system into a crisp control action.

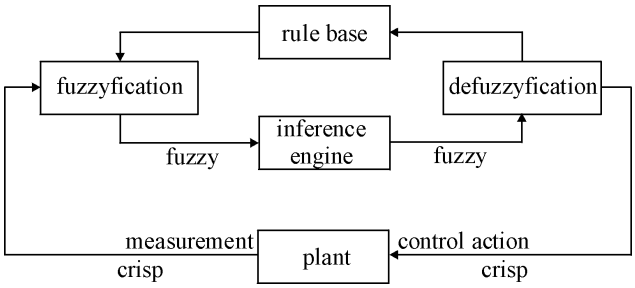

Fig. 9: Fuzzy logic controller (FLC)

The Mamdani-type FLC design is carried out by using the human-operator experience for input-output linguistic (fuzzy) presentation and manual fuzzy rule base formulation, which describes the control philosophy of expert knowledge.

To reduce the steady-state error of the controlled MR shock damper, an FLC with integral behaviour is necessary. Such a PI-FLC observes two input signals: error $e(t) = v_{ref}(t) - v(t)$ and its first derivative $de(t)$ and one output signal: control action $u(t) = I_{set}(t)$. The implementation of "if-then" expert fuzzy rules R carries out the adjustment of $u(t)$:

$$R_i: \text{ if } e(t) \text{ is } A_j \text{ and } de(t) \text{ is } B_k \text{ then } u(t) \text{ is } C_m, \quad (3)$$

where A_i, B_k and C_m are membership functions of the corresponding input-output signales.

The appropriate parameters for the fuzzy membership functions of the input-output signales for the Mamdani-FLC are depicted in Fig. 10. The error $e(t)$ is separated into 8 membership functions, $de(t)$ and $u(t)$ have 9 membership functions with triangular shape. Hence there were formulated 35 fuzzy rules, belonging to the rule base.

The fuzzy inference engine matches the output of the fuzzyfication block with the fuzzy logic rules and performs the fuzzy implication and the approximate reasoning to decide a fuzzy control action. The fuzzy implication was realised by means of the Mamdani implication (Max-Min inference):

$$\mu_i = \min[\mu_{A_j}, \mu_{B_k}], \quad (4)$$

where μ_{A_j}, μ_{B_k} specify the membership values, obtained from the intersection and union operations

upon membership functions A_j and B_k of the input signals $e(t)$ and $de(t)$. Implementing the "center of area"-method for defuzzyfication, the control action $\tilde{u}(t)$ is expressed as:

$$\tilde{u} = \frac{\sum_{p=1}^{q} u_p \mu(u_p)}{\sum_{p=1}^{q} \mu(u_p)}, \qquad (5)$$

where q is the quantisation level of the output signal $u(t)$.

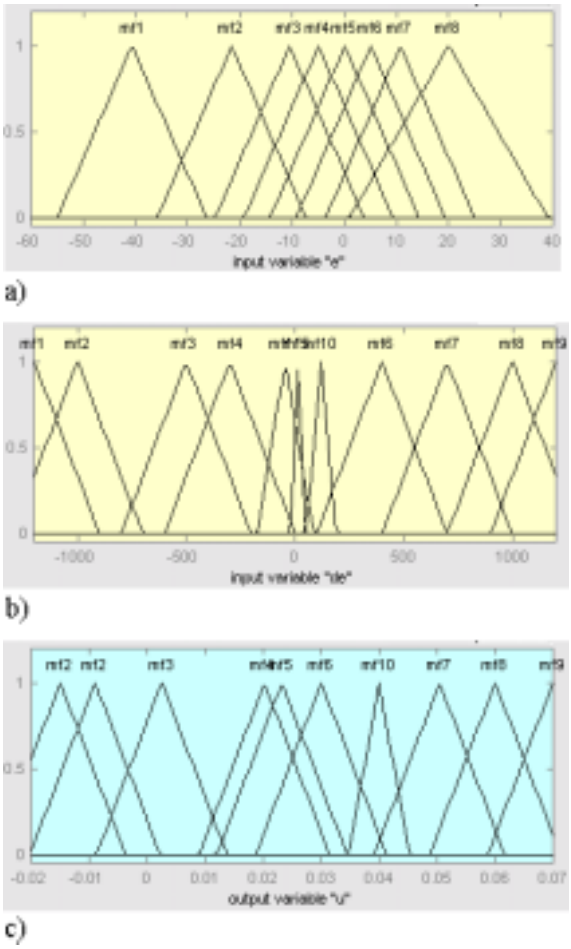

Fig. 10: Mamdani-FLC membership functions of a) $e(t)$, b) $de(t)$ and c) $u(t)$

The transient time T_t of the MR shock damper controlled with the Mamdani-FLC is only 200 ms (Fig. 11). Therefore the Mamdani-FLC is significantly faster than the PI-controller (Fig. 8 a) and the predictive controller (Fig. 8 b). Otherwise, the deviation of the velocity v from the reference signal v_{ref} in Fig. 11 at $t > 2.2$ s is larger than with the PI-controlled damper. A possible reason for these two effects, shorter transient time T_t and larger deviation, is the use of the derivative error $de(t)$ as second input signal. To improve the damper behaviour, more precise expert knowledge has to be involved in the Mamdani-FLC.

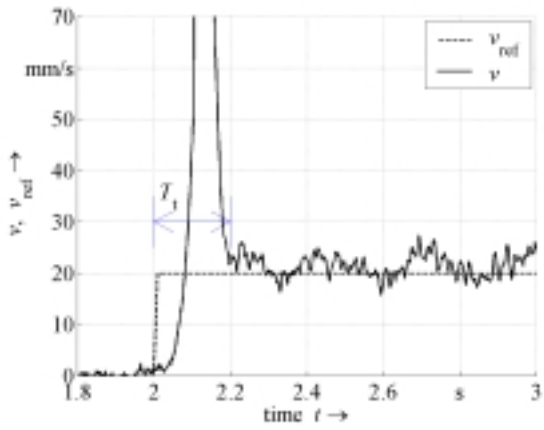

Fig. 11: Step response of the shock damper, controlled with the Mamdani-FLC

In order to adjust precisely and automatically the linguistic rules, connected with the adjustment of membership functions, a Takagi-Sugeno-FLC was designed as a neural network (NN)-based alternative of the conventional Mamdani-FLC design. This second implemented design technique is founded on the known inference system "Anfis" of Jang [9],[10]. The Anfis-based Takagi-Sugeno neuro-fuzzy controller should supply good performance when the training data set is chosen to cover the whole range of the data occuring in use.
Further intentions to reach such good performance are involving more application oriented training data into the FLC design and improving the training algorithm.

4 Vibration Damper

For a variable damping force, e.g. depending on the oscillation frequency of the system, controlled vibration dampers are necessary. Subsequently the controlled vibration damping with MRFs is regarded. Referring to this, an MR vibration damper was developed (Fig. 12). The damper is a cuboid-shaped piston-cylinder construction (Fig. 13). This simplifies the design of the magnetic circuit and ensures that the magnetic flux density B is orthogonal to the MRF flow.
When the piston plunges into the cylinder, the MRF flows upward in the gap of 1 mm between piston and cylinder. In this way the damper uses both the flow and the shear modes. The MR vibration damper shows a high ratio of the damping forces with and without magnetic field and also a very low friction without magnetic field. Therefore it is especially suitable for investigations on oscillating mechanical systems about their eigenfrequency.
In the used oscillating system the vibrations are generated by two counter-rotating masses m_{ex} driven

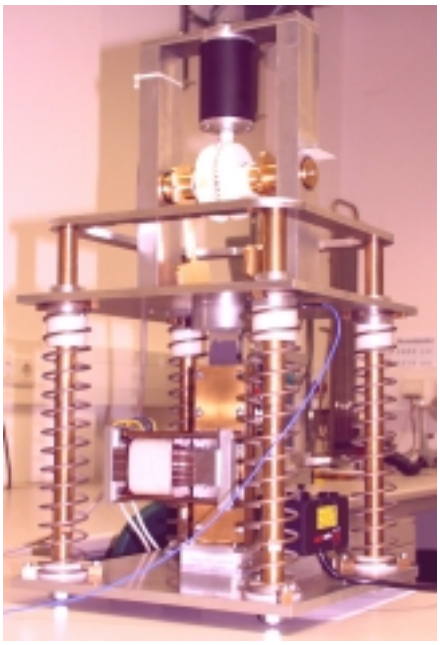

Fig. 12: MR vibration damping system

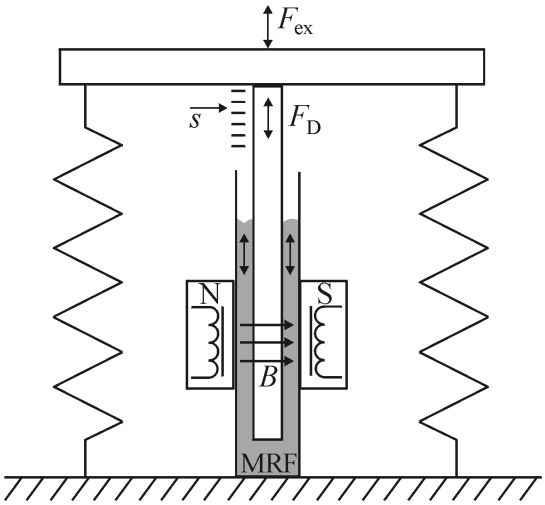

Fig. 13: Scheme of an MR vibration damping system

by an electric motor. The excitation force F_{ex} is

$$F_{ex} = m_{ex} l_{ex} \omega_{ex}^2 \cdot \sin(\omega_{ex} t) \qquad (6)$$

with the eccentricity l_{ex} and the angular frequency ω_{ex}. The motor and the masses m_{ex} are supported on four coil springs. The eigenfrequency f_e of the undamped system is 4.4 Hz.

The difference between the curves in Fig. 14 and the amplitude-frequency response curve of a conventional inertia-force driven system is that the curves in Fig. 14 start for $I > 0$ and thereby for $B > 0$ at frequencies $f > 0$ and not at the point of origin. The reason is the magnetic field-dependent friction $\tau_f(B)$ in (1). In the region around the eigenfrequency f_e the MR-damper works very effective. At higher frequencies f the damping effect concerning the vibration amplitude s decreases. At frequencies $f > 11$ Hz the excitation force F_{ex} is very high so that no difference between the vibration amplitudes s of the damped and the undamped system is measurable. On the other hand, at frequencies $f > \sqrt{2}\, f_e$ the forces acting on the foundation are bigger for the damped system than for the undamped system [11],[12]. To protect the foundation it is advisable to reduce or to switch off the damper at such frequencies. In this case a frequency-dependent controller is necessary.

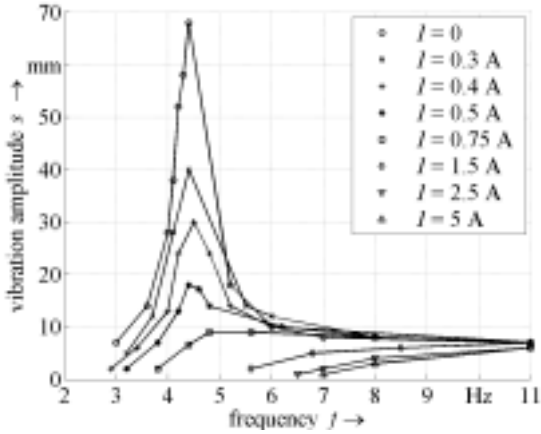

Fig. 14: Amplitude-frequency response curves of the MR vibration damping system at different currents I

The implemented and tested frequency-dependent controller is a well-known P-controller which increases the current I proportionally to a rising vibration amplitude s (Fig. 15).

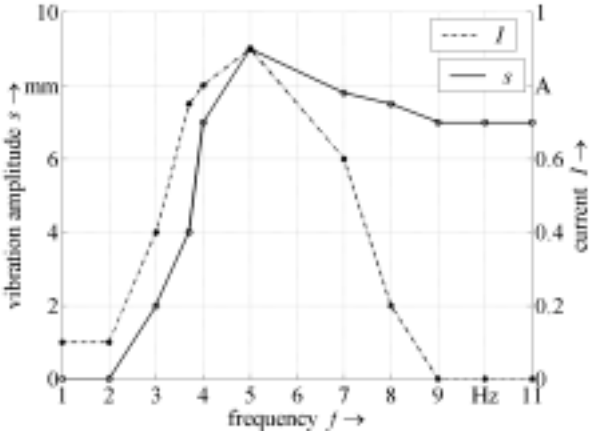

Fig. 15: left ordinate: Amplitude-frequency response curve of the MR vibration damping system with frequency-dependent controller,
right ordinate: Damper current I

In addition to this the influence of the P-controller decreases at frequencies 5 Hz < f < 9 Hz. For frequencies $f > 9$ Hz the current I is switched off and the system oscillates undampedly. In this case the vibration amplitude s is not higher than for the damped system. At frequencies $f < 9$ Hz the damped

vibration amplitude *s* is much smaller than in the undamped case (compare Fig. 14, curve $I = 0$).

The frequency dependent damping with an MR vibration damper is an efficient method for the controlled reduction of vibrations, especially about the eigenfrequency f_e of the system. Interesting applications may be e.g. the damping of machine foundations during the start-up procedure, the damping of washing machines etc.

5 Conclusions

Magnetorheologial fluids are innovative materials which are of particular interest for the development of intelligent dampers. With MRFs the damping force is fast and comfortably modifiable by a magnetic field in a wide range. For an efficient use of this advantage a combination with a continuously working controller is advised.

Two new MR dampers for shock and vibration damping were designed and constructed as well as different types of controllers and their behaviour in connection with the MR dampers were presented. The shock damper provides a damping force of about 1 kN in a very energy-efficient way. The vibration damper reduces the vibration amplitude of an oscillating system about its eigenfrequency f_e from approximately 70 mm down to nearly zero.

The potential applications of MR dampers in the mechanical and vehicle engineering are advancing rapidly. In the next future the step from special applications, e.g. in truck seats and in knee prostheses, to an usage in mass products, especially in the vehicle engineering, could be expected.

References:

[1] Ashour, O., C. A. Rogers, W. Kordonsky: Magnetorheological Fluids: Materials, Characterisation and Devices, *Journal of Intelligent Material Systems and Structures*, **7** (March 1996), pp. 123-130.

[2] Kordonsky, W.: Elements and Devices Based on Magnetorheological Effect, *Journal of Intelligent Material Systems and Structures*, **4** (1993), pp. 65-69.

[3] Richter, L., L. Zipser, U. Lange: Properties of Magnetorheological Fluids, *Sensors and Materials*, Vol. **13**, No. 7 (2001), pp. 385-397.

[4] Grasselli, Y., G. Bossis, E. Lemaire: Field Induced Structure in Magnetorheological Suspensions, *6th European Colloid and Interface Society Conf.*, 1993, pp. 175-177.

[5] Carlson, J. D., B. F. Spencer Jr.: Magneto-rheological Fluid Dampers for Semi-Active Control, *Proceedings of the 3rd International Conference on Motion and Vibration Control*, Japan, Vol. **3**, (Sept. 1996), pp. 35-40.

[6] Jolly, M. R., J. D. Carlson, B. C. Munoz: A Model of the Behaviour of Magnetorheological Materials, *Journal of Smart Materials and Structures*, **5** (1996), pp. 607-614.

[7] Zipser, L., L. Richter, U. Lange: Magnetorheologic Fluids for Actuators, *14th European Conference on Solid-State Transducers*, Copenhagen, Denmark, August 27 - 30, 2000, pp. 667-670.

[8] Nie, J., D. A. Linkens: *Fuzzy-Neural Control, Principles, Algorithms and Applications*, Prentice Hall, New York, 1995.

[9] Jang, J.-S. R.: ANFIS: Adaptive-Network-Based FIS. *IEEE Trans. Systems, Man and Cybernetics*, **23** (03) 1993, pp. 665-685.

[10] Jang, J.-S. R., C. T. Sun: Neuro-Fuzzy Modelling and Control, *IEEE*, **83** (3) 1995, pp. 379-406.

[11] Jürgler, R: *Maschinendynamik*, VDI-Verlag, Düsseldorf, 1996.

[12] Tongue, B. H.: *Principles of Vibration*, Oxford University Express, New York, 1996.